A novel image fusion algorithm based on bandelet transform

Xiaobo Qu (屈小波)[1], Jingwen Yan (闫敬文)[2,1], Guofu Xie (谢国富)[3],
Ziqian Zhu (朱自谦)[4], and Bengang Chen (陈本刚)[4]

[1]*Department of Communication Engineering, Xiamen University, Xiamen 361005*
[2]*Department of Electronic Information Engineering, Shantou University, Shantou 515063*
[3]*Department of Software Engineering, Xiamen University, Xiamen 361005*
[4]*Research Institute of Chinese Radar Electronic Equipment, Wuxi 214063*

A novel image fusion algorithm based on bandelet transform is proposed. Bandelet transform can take advantage of the geometrical regularity of image structure and represent sharp image transitions such as edges efficiently in image fusion. For reconstructing the fused image, the maximum rule is used to select source images' geometric flow and bandelet coefficients. Experimental results indicate that the bandelet-based fusion algorithm represents the edge and detailed information well and outperforms the wavelet-based and Laplacian pyramid-based fusion algorithms, especially when the abundant texture and edges are contained in the source images.

OCIS codes: 100.0100, 100.7410, 350.2660, 350.6980.

Image fusion is the combination of two or more different images to form a new image by using a certain algorithm[1]. The combination of sensory data from multiple sensors can provide more reliable and accurate information. It forms a rapidly developing research area in remote sensing, medical image processing, and computer vision[2−4]. Most of these approaches were based on combining the multiscale decompositions (MSDs) of the source images. MSD-based fusion schemes provide much better performance than the simple methods studied previously[4,5]. Due to joint information representation at the spatial-spectral domain, the discrete wavelet transform (DWT) becomes the most popular approximation in image fusion. The human visual system is especially sensitive to local contrast changes, i.e., edges. Rapid contrast changes contain extremely useful information for the human observer. Unfortunately, wavelets cannot take advantage of the geometrical regularity of image structures[6]. Sharp image transitions such as edges are expensive to represent, although one could reduce their cost by taking into account the fact that they often have a piecewise regular evolution across the image support[7]. Bandelet transform is an analysis tool which aims at taking advantage of sharp image transitions in images. A geometric flow, which indicates directions in which the image gray levels have regular variations, is used to form bandelet bases in bandelet transform. The bandelet bases lead to optimal approximation rates for geometrically regular images and are proven to be efficient in still image compression, video compression, and noise-removal algorithms[8−10].

Apparently, bandelet transform is appropriate for the analysis of edges and texture of images. When introducing bandelet transform to image fusion, one can take the features of source images well and provide more information for fusion. In our experiment, the fused image with the proposed bandelet-based fusion algorithm could represent the edge and detailed information as the original images. Compared with wavelet-based and Laplacian pyramid-based algorithms, bandelet-based algorithm leads to better fusion result.

In bandelet transform, a geometric flow of vectors is defined to represent the edges of image. These vectors give the local directions in which the image has regular variations. Orthogonal bandelet bases are constructed by dividing the image support in regions inside which the geometric flow is parallel. Let Ω_i denote the ith region, which composes the image support $S = \cup_i\Omega_i$. Within each Ω_i the flow is either parallel horizontally or vertically. Figure 1 shows an example of a vertically parallel geometric flow in a region of the hat of Lena image.

The image is partitioned small enough into square regions, each region Ω_i includes at most one contour. If a region does not include any contour, the image intensity is uniformly regular and the flow is not defined. In bandelet transform, these regions are approximated in the separable wavelet basis of $L^2(\Omega)$ in

$$\left\{ \begin{array}{c} \phi_{j,m_1}(x_1)\psi_{j,m_2}(x_2) \\ \psi_{j,m_1}(x_1)\phi_{j,m_2}(x_2) \\ \psi_{j,m_1}(x_1)\psi_{j,m_2}(x_2) \end{array} \right\}_{(j,m_1,m_2)\in I_\Omega}, \qquad (1)$$

where I_Ω is an index set that depends upon the geometry of the boundary of Ω, and x_1, x_2 denote the location of pixel in the image, $\phi_{j,m_1}(x_1)\psi_{j,m_2}(x_2)$,

Fig. 1. Geometric flow of the hat of Lena.

© 2007 Chinese Optics Letters

$\psi_{j,m_1}(x_1)\phi_{j,m_2}(x_2)$, and $\psi_{j,m_1}(x_1)\psi_{j,m_2}(x_2)$ are the modified wavelets at the boundary. If a geometric flow is calculated in Ω, this wavelet basis is replaced by a bandelet orthonormal basis of $L^2(\Omega)$ in

$$
\left\{
\begin{array}{c}
\phi_{l,m_1}(x_1)\,\psi_{j,m_2}(x_2-c(x_1)) \\
\psi_{j,m_1}(x_1)\,\phi_{j,m_2}(x_2-c(x_1)) \\
\psi_{j,m_1}(x_1)\,\psi_{j,m_2}(x_2-c(x_1))
\end{array}
\right\}_{j,l>j,m_1,m_2}, \quad (2)
$$

which is got by inserting bandelets in the warped wavelet basis in

$$
\left\{
\begin{array}{c}
\phi_{j,m_1}(x_1)\,\psi_{j,m_2}(x_2-c(x_1)) \\
\psi_{j,m_1}(x_1)\,\phi_{j,m_2}(x_2-c(x_1)) \\
\psi_{j,m_1}(x_1)\,\psi_{j,m_2}(x_2-c(x_1))
\end{array}
\right\}_{(j,m_1,m_2)\in I_{W\Omega}}. \quad (3)
$$

In the above expressions, $c(x)$ denotes a flow line associated to a fixed translation parameter x_2, $(x_1, x_2 + c(x_1)) \in \Omega$ is a set of point for x_1 varying, and l is the direction of geometric flow which is more elongated $(2^l > 2^j)$ and $c(x)$ is defined as

$$
c(x) = \int_{x_{\min}}^{x} c'(u)\,\mathrm{d}u. \quad (4)
$$

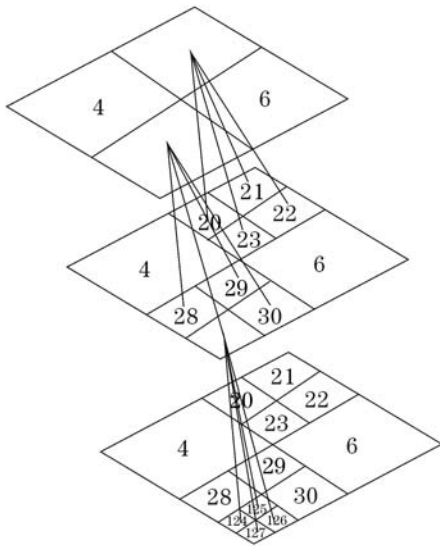In the bandelet representation, the M parameters

Fig. 2. Quad tree of dyadic square image segmentation.

include the bandelet coefficients used for computing and the parameters that specify the image partition and the geometric flow in square regions, which are subdivided into four smaller squares, corresponding to a node having four children in the quad tree, as shown in Fig. 2. In order to achieve appropriate image geometry of image f, the best geometry is employed to an approximation f_M from M parameters that minimize the approximation error $||f - f_M||$.

In each region Ω_i of the segmentation, one must decide if there should be a geometric flow. If this flow is parallel, $c'(t)$ is calculated as an expansion over translated B-spline functions dilated by a scale factor 2^l. Over a square Ω of width, the flow at a scale 2^l is characterized by 2^{k-l} coefficients α_n,

$$
c'(t) = \sum_{n=1}^{2^{k-l}} \alpha_n b\left(2^{-l}t - n\right). \quad (5)
$$

The scale parameter 2^l is adjusted through a global optimization of the geometry. When the image f has contours that are curves C^α which meet at corners or junctions, and that f is C^α away from these curves, this procedure leads to a bandelet approximation that has an optimal asymptotic error decay rate R

$$
R = ||f - f_M||^2 \le CM^{-\alpha}, \quad (6)
$$

although α is unknown.

In the bandelet-based fusion algorithm, bandelet transform is used as a MSD tool for images. It can extract the features of original images well, such as edges and texture, so that more information is provided for fusion.

The fusion framework using bandelet transform is shown in Fig. 3. The operational procedure for the proposed bandelet-based image fusion approach is given as follows.

1) The two source images in the fusion are geometrically registered to each other.

2) Compute the image sample values along the flow lines in each region Ω_i of the partition.

3) Geometric flow $G_j(i)$ $(j = 1, 2, \cdots, N)$ in each region Ω_i and bandelet coefficients $C_j(x, y, i)$ $(j = 1, 2, \cdots, N)$ corresponding to the geometric flow are computed. N is the total number of source images,

C_1, C_2: bandelet coefficients of source images
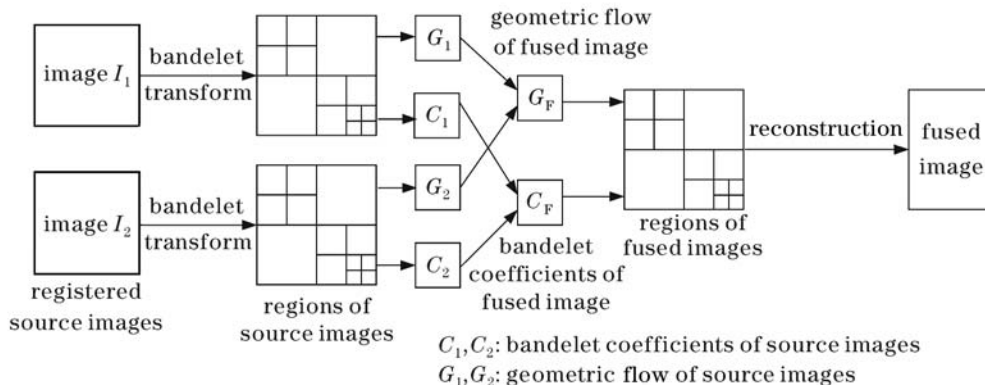G_1, G_2: geometric flow of source images

Fig. 3. Fusion framework using bandelet transform.

$C_j(x, y, i)$ is the bandelet coefficient of jth source image at the pixel (x, y) and $(x, y) \in \Omega_i$.

4) Process the fusion rules. For the geometric flow, fusion with the maximum rule

$$G_{\mathrm{F}}(i) = \begin{cases} G_1(i), & \text{if} \quad G_1(i) \geq G_2(i) \\ G_2(i), & \text{if} \quad G_1(i) < G_2(i) \end{cases}. \qquad (7)$$

For the bandelet coefficients, fusion with the maximum absolute value rule:

$$C_{\mathrm{F}}(x, y, i) = \begin{cases} C_1(x, y, i), & \text{if } \mathrm{abs}(C_1(x, y, i)) \\ & \geq \mathrm{abs}(C_2(x, y, i)) \\ C_2(x, y, i), & \text{if } \mathrm{abs}(C_1(x, y, i)) \\ & < \mathrm{abs}(C_2(x, y, i)) \end{cases}. \qquad (8)$$

In expressions (7) and (8), $G_{\mathrm{F}}(i)$ denotes the geometric flow in the region Ω_i of the fused image, $C_{\mathrm{F}}(x, y, i)$ is the bandelet coefficient of fused image at the pixel (x, y) and $(x, y) \in \Omega_i$.

5) The fused image is reconstructed by the bandelet inverse transform using geometric flow $G_{\mathrm{F}}(i)$ and bandelet coefficients $C_{\mathrm{F}}(x, y, i)$.

The performance evaluation criteria of image fusion are still a hot topic in the research of image fusion[4]. Besides visual observation, objective performance evaluation criteria are used in this paper, such as the standard deviation, average gradient, entropy, and mutual information[11,12]. To evaluate the performance of the proposed fusion algorithm, we compare in with two typical algorithms: the maximum algorithm based on wavelet transform and the maximum algorithm based on Laplacian pyramid which was summarized in Ref. [4].

In the experiment, two blurred images are used as source images, as shown in Fig. 4. The source images are 256×256 in size and 256 levels in gray value. It can be seen that Fig. 4(a) is clear in circumjacent region around the center of the image and blurred in the center region. In contrast, Fig. 4(b) is clear in the center region and blurred in circumjacent region. Our aim is to obtain a totally clear image. The fusion results of different algorithms are shown in Fig. 5 and the objective performance evaluation criteria are compared in Table 1.

Figure 5(a) shows the fused image obtained by the proposed bandelet-based algorithm. From the visual observation of the fusion results, the bandelet-based fused image is clearer and contains more detailed and texture features than the wavelet-based and Laplacian pyramid-based fused images. Figures 5(d)—(i) are the difference between source images and fused images of three fusion algorithms. By examining the differences, we can see that the bandelet-based fused image nearly extracts

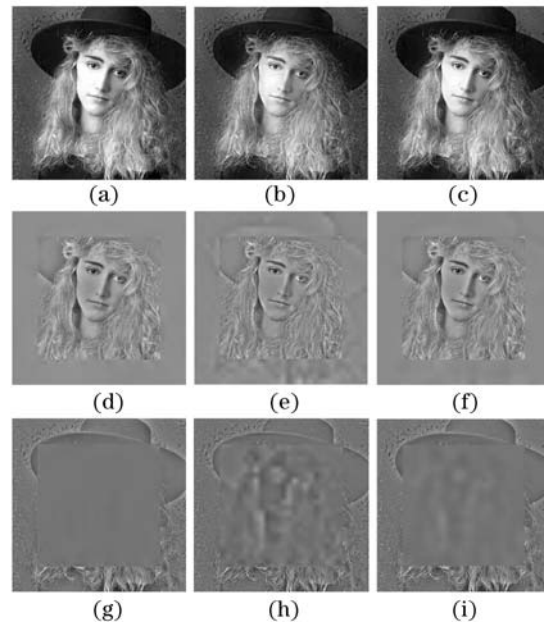Fig. 4. Source images in the fusion experiment.

Fig. 5. Fusion results using different algorithms. (a)—(c) Fused images obtained by the bandelet-based algorithm, the wavelet-based algorithm, and the Laplacian pyramid-based algorithm; (d)—(f) differences between the fused image and source image of Fig. 4(a) for the bandelet-based algorithm, the wavelet-based algorithm, and the Laplacian pyramid-based algorithm; (g)—(i) differences between the fused image and source image of Fig. 4(b) for the bandelet-based algorithm, the wavelet-based algorithm, and the Laplacian pyramid-based algorithm.

Table 1. Objective Performance Evaluation Criteria of Different Algorithms

Algorithm	Bandelet	Wavelet	Laplacian
Standard Deviation	63.3180	59.934	61.9693
Average Gradient	18.1056	17.9613	18.0568
Entropy	7.7470	7.7313	7.7368
Mutual Information	6.2880	4.7781	5.6485

almost all clear parts in source images, especially in the face edges and hair part of the girl. It proves that bandelet represents edges better than wavelets and Laplacian pyramid, especially when the source images contain abundant texture features.

In Table 1, all objective performance evaluation criteria of bandelet-based algorithm outperform the other two typical algorithms. Larger standard deviation and entropy indicate that more information is contained in the bandelet-based fused images. Larger average gradient indicates richer detailed information. Larger mutual information proves that bandelet-based fused image is strongly correlated with the source images and more image features are preserved in the fusion. Therefore, from the subjective and objective analyzes, the proposed algorithm gives better performance than the other two algorithms. Bandelet-based algorithm is optimal for image fusion, especially when abundant texture features are contained in the source images.

Bandelet transform is an efficient analysis tool to take advantage of sharp image transitions in images and can

take the image feature well, especially the abundant texture and edges. From the visual observation, the bandelet-based fused image has clear edge and texture, image features from source images are extracted and reserved well. Objective performance evaluation criteria also prove that bandelet-based fusion algorithm can offer better performance than the wavelet-based and Laplacian pyramid-based fusion algorithms. The bandelet-based algorithm will have a bright future in fusion field, especially when abundant texture features are contained in the source images.

Because the bandelet transform is newly introduced into the image fusion field, much work are needed. From our experiment, we can expect the following extension of research in this area. 1) Other fusion rules could be employed, no only the maximum rule. 2) The combination of geometric flow and bandelet coefficients for fusion could be considered. 3) Fast algorithm of bandelet transform needs further investigation.

References

1. D. L. Hall and J. Llinas, Proceedings of the IEEE **85**, 6 (1997).
2. C. Pohl and J. L. Van Genderen, Intl. J. Remote Sensing **19,** 823 (1998).
3. C. S. Pattichis, M. S. Pattichis, and E. Micheli-Tzanakou, in *Proceedings of 35th Asilomar Conference on Signals, Systems, and Computers* 1263 (2001).
4. Z. Zhang and R. S. Blum, Proceedings of the IEEE **87,** 1315 (1999).
5. C. Liu, Z. Jing, G. Xiao, and B. Yang, Chin. Opt. Lett. **5,** 274 (2007).
6. H. Li, L. Guo, and H. Liu, Acta Opt. Sin. (in Chinese) **26,** 657 (2006).
7. E. Le Pennec and S. Mallat, IEEE Trans. Image Processing **14,** 423 (2005).
8. G. Peyré and S. Mallat, ACM Trans. Graphics (SIG-GRAPH'05) **14,** 601 (2005).
9. O. Alatas, O. Javed, and M. Shah, IEEE Trans. Image Processing **15,** 3812 (2006).
10. X. Yang, L. Jiao, and W. Li, Acta Electron. Sin. (in Chinese) **34,** 2063 (2006).
11. H. Wan, J. Peng, and W. Wu, J. Infrared and Laser Engineering (in Chinese) **33,** 189 (2004).
12. G. Qu, D. Zhang, and P. Yan, Electron. Lett. **38,** 313 (2002).